CHEMICAL AND STRUCTURAL ANALYSIS OF CERAMIC POWDERS USED IN CONTINUOUS CASTING PROCESS

L. Roldo[I], P. H. S. Cardoso[II], C. A. M. Moraes[III], F. A. de Oliveira Neto[III], T. R. Strohaecker[IV], A. C. F. Vilela[IV]

[I] Materials Department, Federal University of Rio Grande do Sul. Av. Osvaldo Aranha, 99/604, Porto Alegre, RS, 90035-190, Brazil
e-mail: liane.roldo@ufrgs.br

[II] Manufacturing and Materials Group, University of Rio Grande.

[III] Materials Characterization Research Group, University of Vale do Rio dos Sinos.

[VI] Metallurgy Department, Federal University of Rio Grande do Sul.

Abstract

Three different ceramic powders used in continuous casting process were analyzed in three different conditions. The conditions were: the original powder (collected in the steel mill storage), the original dried powder, to simulate the powder condition just before use in casting process and the melted powder, to reproduce the powder condition after the passage of the molten steel. X-ray Diffraction, micro-Raman spectroscopy and X-ray Fluorescence were carried out to investigate the chemical features of the material. Thermogravimetric and Differential Thermal Analysis were employed as well to evaluate the structural behavior of the powders under heating. A considerable qualitative phase composition was obtained for each sample condition. Wollastonite ($CaSiO_3$) was the major phase identified in the original powders, and in the melted powders the major phase was cuspidine ($Ca_4Si_2O_7F_2$).

Keywords: ceramic powder, continuous casting, wollastonite, cuspidine

1 Introduction

Due to the demand for efficiency of the continuous casting process, the determination of ceramic powders chemical and structural characteristics plays a significant role in the steelmaking process. An inappropriate flux powder selection can lead to tremendous liabilities associated with safety, equipment damage, and loss of productivity, resulting in unfavourable customer perception [1].

Ceramic powders or mould fluxes are synthetic slag, which cover the liquid pool surface during the continuous casting of steel [2]. Several studies have shown that the slag film formed between mould and strand contains three layers: a glassy zone close to the mould, a crystalline layer in the centre and a liquid film in contact with the steel [3,4]. The basic functions of ceramic powders are: to provide lubrication between the strand and the mould, to moderate heat transfer between the mould and the strand, to prevent oxidation, to provide thermal insulation, and to act as reservoir for the absorption of inclusions, both solid and liquid [5] .

In general, inappropriate ceramic powder application can cause several problems [5-7]. Those problems can be surface cracking, sub-surface cleanliness problem on the castings, slag patches on the surface of continuous cast sections, chemical interaction between the liquid steel and the liquid mould flux, and environmental problems due to the instability of fluxes at high temperatures, releasing gaseous fluorine, a toxic chemical element, in the atmosphere.

The main components usually present in ceramic powders are: quartz (SiO_2), lime (CaO), sodium oxide (Na_2O), fluorite (CaF_2), and carbon (C) [8-11]. Other components that eventually appear in reasonable amounts are alumina (Al_2O_3), burnt magnesite (MgO), some alkaline oxides (K_2O, LiO_2), and some metal oxides of iron, manganese, and titanium.

X-ray diffraction analysis has shown that many of these components are present as more complex phases, e.g., wollastonite ($CaSiO_3$), limestone ($CaCO_3$), sodium carbonate (Na_2CO_3), sodium fluoride (NaF), and cuspidine ($Ca_4Si_2O_7F_2$)[12]. The phases complexity can be easily seen in the case of carbon, which may be added to the original powder as coke dust, lampblack, graphite, or fly ash, or even as calcium and sodium carbonate [13]. Further findings have shown that phases like cuspidine, nepheline ($NaAlSiO_4$) and a sodium silicate (Na_2SiO_3) play an important role in the heat transfer from the strand to the mould in the production of different

steel grades [10]. The primary aim of the work is to identify the chemical and structural composition of three ceramic powders used in steel continuous casting equipment. The correct identification of components is important to optimize the fluxes fabrication and for further improve of their basic industrial functions.

2 Experimental

Three different powders I, J and K were analysed in three different conditions. Such conditions were: the original powder (collected in the steel mill before use), the original powder dried at 120 °C for 24 hours and, 20 g of the original fluxes were melted in a graphite crucible by using a laboratory electrical resistance furnace. These samples were heated up till 1500 °C, maintained at the temperature for 30 minutes, plus 2 hours of soaking time and cooled down slowly inside the furnace.

Each powder was crushed in an alumina crucible and sifted in a 100-mesh screen before any analysis. The mould fluxes chemical composition analyses were carried out using: X-ray Fluorescence (XRF, Philips PW-2600, with a standard pattern), X-ray Diffraction (XRD, Cukα Philips X'Pert MPD Diffractometer with monochromator and proportional detector) with 4 seconds per step of 0.02 degrees and spinning speed (when employed) of 1 rev/s, Micro-Raman Spectroscopy (Dilor LabRam, ISA Jobin-Yvon micro-Raman in range of 100-1700 cm^{-1}, 20 mW HeNe laser λ = 632.817 nm) coupled to an optical microscope Olympus BX40. The thermal stability of dried mould powder was obtained by using a Thermogravimetric and a Differential Thermal Analyzer (TG, DTA - NETZSCH STA 409C Thermal Analysis). The TG and DTA analysis were carried out using a platinum-iridium crucible containing 0.100 g of powder heated up to 1450 °C under a nitrogen atmosphere by pouring 50 ml of N_2. The heating up and cooling down rates were 10 °C/min.

3 Results and Discussion

Tables 1 and 2 present the results of the X-ray fluorescence chemical analysis for the original and the melted powder, respectively. The carbon values should be taken only as qualitative results because carbon can be burnt during the sample drying step prior the analysis.

XRF analysis was employed because it is an adequate technique as primary rough chemical analysis, and the most common technique employed in the industry to determine the chemical composition of ceramic powders [13].

Table 1 - X- Ray Fluorescence chemical analysis of original ceramic powders (wt %).

	CaO	SiO_2	MgO	Al_2O_3	FeO	Na_2O	K_2O	C	Cr_2O_3	TiO_2
I	28.9	32.0	2.6	5.6	2.83	7.23	0.85	18	0.22	0.49
J	26.5	40.2	1.5	3.55	1.58	4.76	0.16	20	0.23	0.28
K	37.9	36.7	0.8	3.3	0.9	7.20	0.13	3.6	0.15	0.1

Table 2 - X- Ray Fluorescence chemical analysis of melted powders (wt %).

	CaO	SiO_2	MgO	Al_2O_3	FeO	Na_2O	K_2O	C	Cr_2O_3	TiO_2
I	32.5	45.5	2.95	8.30	1.66	2.22	0.39	0.15	0.15	0.42
J	42.78	40	1.75	8.36	1.22	0.94	0.11	0.05	0.18	0.30
K	40.12	41.62	1.32	5.54	0.97	1.88	0.06	0	0.14	0.10

It can be observed that Na_2O, K_2O, and C amounts decreased when the samples were melted, suggesting that those elements were removed during the heating up. Such tendency will be confirmed using X-ray diffraction analysis.

Figure 1 shows the X-ray diffraction pattern of powder I in the original and melted conditions. In the original analysis, spinning was applied to the sample holder due to the powders non-uniformities. With the spinning movement the area exposed to X-ray beam was continuously changed during the analysis. In fact, the spinning on the original powder was necessary because, according to the Joint Committee on Powder Diffraction Standards (JCPDS) software, several peaks from important phases presented much higher intensity than expected in 2θ positions [14]. This feature is related to the absence of homogeneity in the powders, i.e., some grains from a specific phase could be in a favourable orientation according to the diffraction axes. After spinning, the resultant area generated by the Lorentz and Gauss fitting gave a good explanation for the overlapping peaks.

The second step was to submit the original powders to a drying process. The purpose was to avoid wrong phase's identification due to hydration. Nevertheless, the relative intensity of some peaks decreased and some others increased, and the

XRD results were the same as the original powder. As a result, those analyses were not presented in this work.

In the original powder I (Figure 1a), the main encountered elements are in agreement with the indicative results obtained by X-ray fluorescence analysis. Those elements were distributed in the following phases: (1) $CaSiO_3$ (wollastonite), (2) SiO_2 (quartz), (3) CaF_2 (fluorite), (4) $CaCO_3$ (calcium carbonate) and (5) Na_2CO_3 (sodium carbonate). The same approach was employed to the other two powders (J and K). Figure 2 and 3 show the XRD from powders J and K. The encountered phases were the same, as those encountered in powder I plus (6) Na_2SiF_6 (malladrite) and (7) $CaSO_4$ (calcium sulphide).

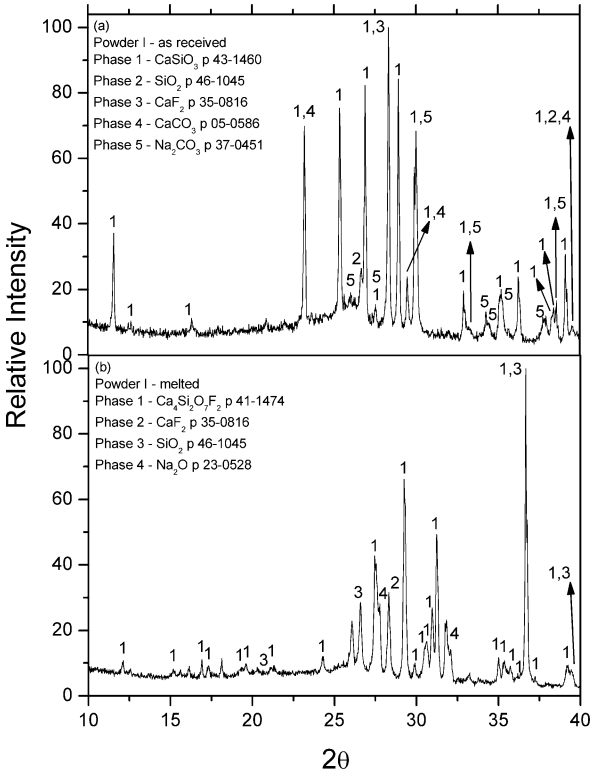

Figure 1 - (a) XRD with spinning of the original powder I, and, (b) XRD of the melted powder I.

The wollastonite present in all XRD patterns was identified as belonging to monoclinic system, and such phase was in best agreement with the X-ray patterns. However, according to the literature, the most common wollastonite phase is triclinic [13]. The JCPDS pattern for the triclinic phase could also be a good pattern for all cases, though it can be possible this phase was also present.

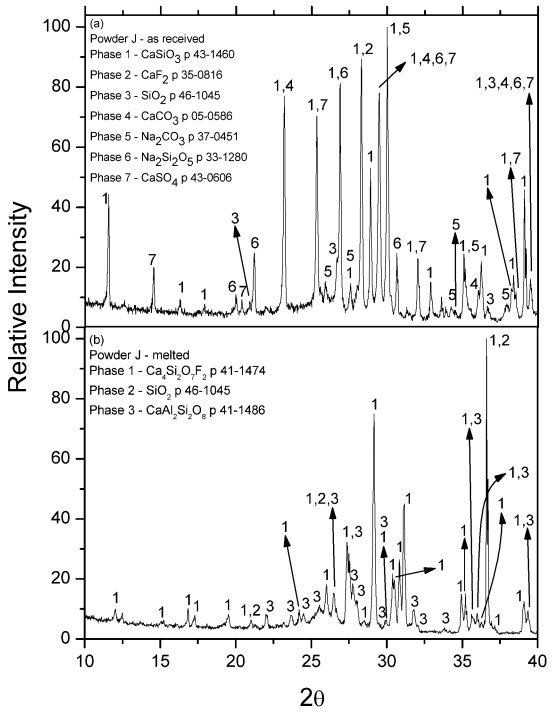

Figure 2 - (a) XRD with spinning of the original powder J, and (b) XRD of the melted powder J.

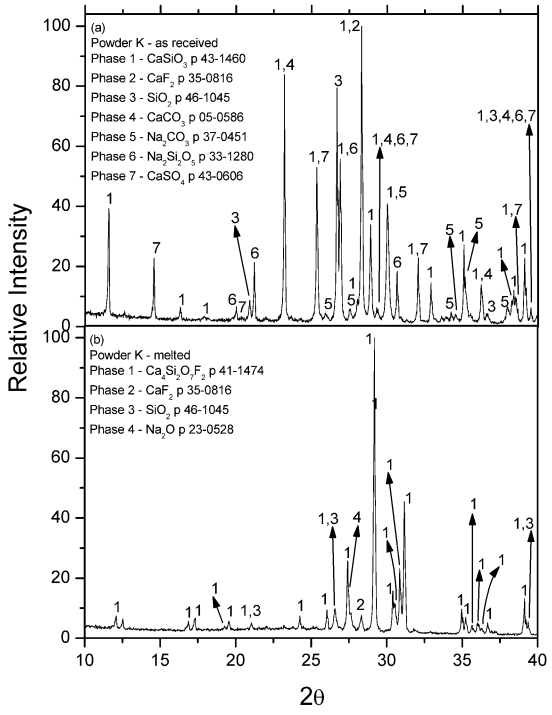

Figure 3 - (a) XRD with spinning of the original powder K, and (b) XRD of the melted powder K.

Wollastonite seems to be the one present in the highest amount. For this phase a preferential X-ray diffraction orientation was found in the direction (200). Even though CaF_2 was not analysed via XRF, it seems that fluorite is very detectable via XRD (Figure 1a, phase 3, hkl 111). This phase was identified as belonging to the cubic system.

The diffraction patterns, of the original powders, in Figure 1a, 2a, and 3a indicate the presence of amorphous phase belonging probably to aluminium or silicon compounds, which was expected.

The main identified component in the XRD analysis for the melted powders (Figure 1b, 2b, and 3c) was cuspidine ($Ca_4Si_2O_7F_2$). CaF_2 and SiO_2 phases, which are responsible for the formation of cuspidine, from the original diffraction pattern (unmelted state) were also observed showing that the reactions were not complete under the experimental conditions.

An amorphous phase, probably related to Al based oxides, was also detected in the melted condition. However, in powder J, a crystalline phase containing aluminium was detected ($CaAl_2SiO_2$).

As is presented in Figure 4, micro-Raman spectroscopy was also applied in the powders analysis, both in the original and the melted condition (Figure 5).

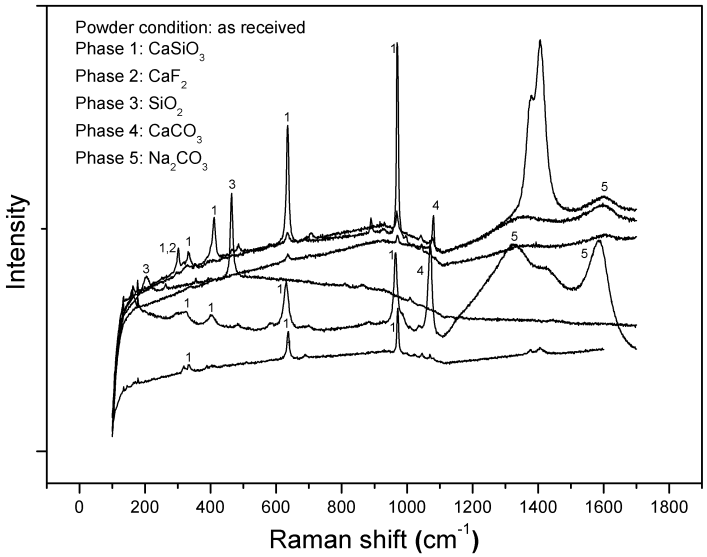

Figure 4 - Raman spectra of the original powders.

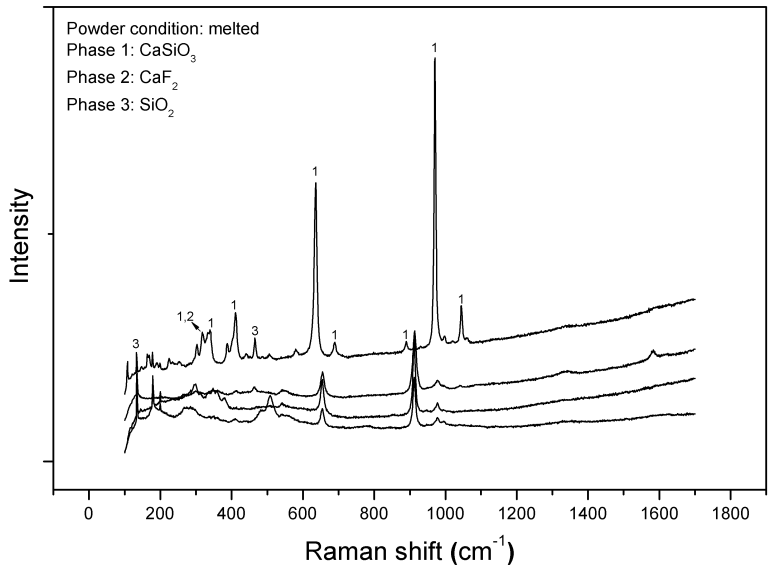

Figure 5 - Raman spectra of the melted powders.

In order to comprehend Raman spectra two issues shall be taken in account:

1. Due to the heterogeneity of the powders and the small area available for analysis, the Raman powders spectra could not confirm all the phases found in each sample for both conditions;

2. Because of the heterogeneity of the powders, different regions of the original and melted powders were randomly analysed (Figure 4 and 5).

For the original condition traces of $CaSiO_3$, CaF_2, SiO_2, $CaCO_3$ and Na_2CO_3 were found on the random Raman spectra in Figure 4 (where the numbers on the peaks follow the diagram phase index).

Figure 5 Raman spectra of melted condition, indicates the presence of $CaSiO_3$, CaF_2 and SiO_2. Although the X-ray diffraction technique did not confirm the presence of $CaSiO_3$ the Raman spectra have shown some remaining wollastonite from the melting process. There were some unidentified peaks that might be cuspidine. The cuspidine presence in the samples via Raman technique could not be evaluated because it was not possible to find a Raman pattern in the literature, nor was it possible to find pure cuspidine to obtain a proper pattern.

The pure phase Raman spectra patterns of $CaSiO_3$, SiO_2, CaF_2, $CaCO_3$ and hydrated Na_2CO_3 (Figure 6) were determined. The pure phase Raman patterns were confirmed as pure ones by both X-ray diffraction and comparison with Atlas database for Raman analysis [15].

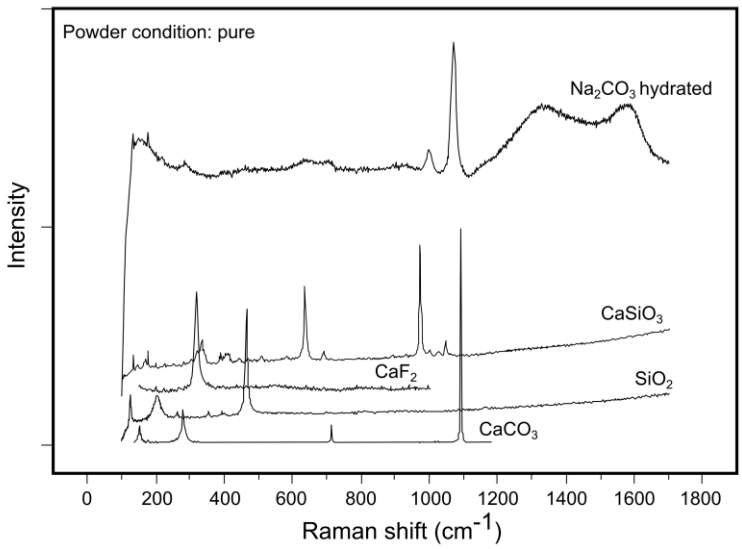

Figure 6 - Raman spectra of the pure phases found in the original and melted conditions.

The Raman characterization results may be very useful because sometimes the same phases from the original powder can be retained in the steel as non-metallic inclusions. If the Raman powder phase spectra are obtained before and after melting, it is possible to compare these spectra with those found in the inclusion after continuous casting process. This technique can give a good indication of the presence of the phase and also the origin of the inclusion.

The thermogravimetric (TG) analysis of the powders under nitrogen atmosphere (Figure 7) confirms, by the mass loss of both powders, the decreasing tendency of C and Na amounts, which was already pointed out elsewhere in the discussion. The mass loss observed in all samples indicates that some elements or compounds can be, essentially, volatilized at temperatures ranging from 400 to 800 °C, which is shown by the several endothermic peaks determined via DTA (Figure 8) in this temperature range.

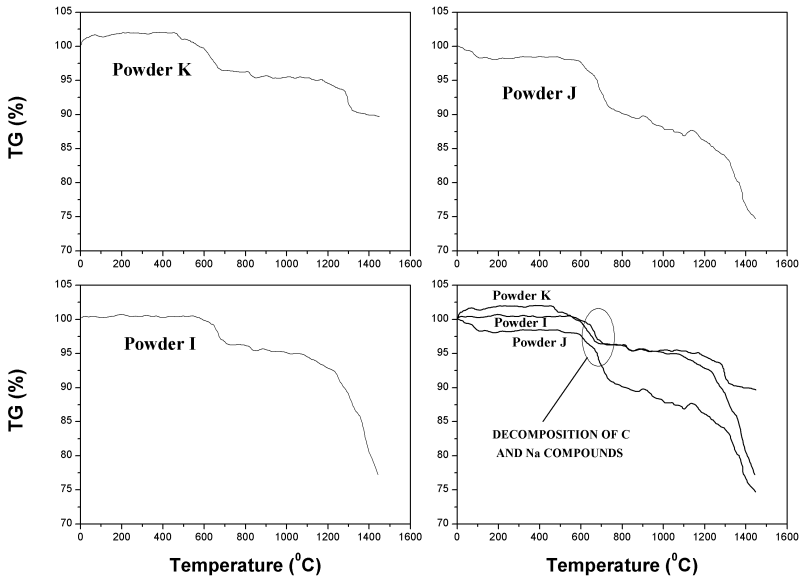

Figure 7 - Thermogravimetric (TG) diagram of powders I, J and K - under nitrogen atmosphere.

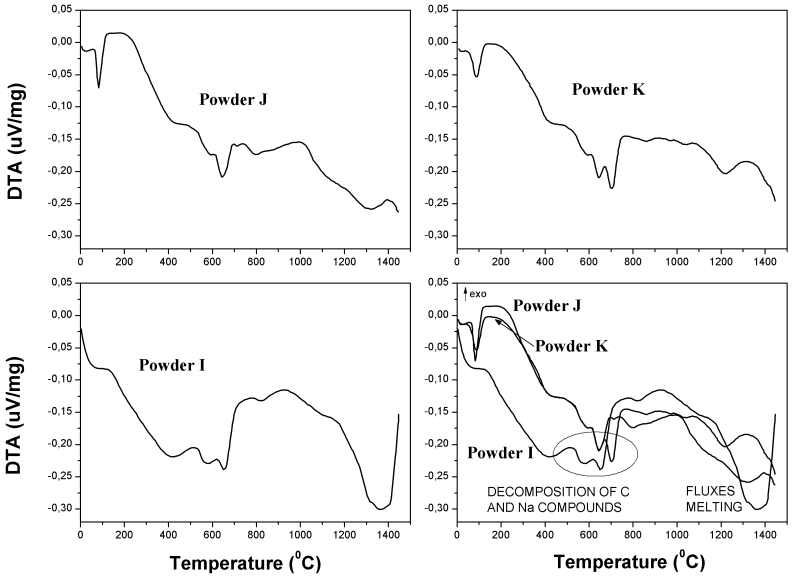

Figure 8 - Differential Thermal Analysis (DTA) diagram of powders I, J and K under nitrogen atmosphere.

It is known that $CaCO_3$ decomposes in the temperature range specified above. As a result of that, the decrease of C observed in the chemical analysis (Tables 1 and 2) is in part due to the decomposition of $CaCO_3$ and $NaCO_3$ with the formation of CO_2. In the case of Na, it is known that this element volatilizes at 885 °C, so the

lower amount encountered in the melted powders suggest its volatilization. TG analysis also confirms that sample K (original powder) is the one with the lowest initial amount of C (chemical analysis from Table 1), resulting in the lowest mass loss between the powders during the heating up to 1450 °C. This tendency was also confirmed by the X-ray diffraction of powder K (Figure 3b) that showed the absence of $CaCO_3$ and a very low presence of Na compound in the melted powder.

4 Conclusions

Sodium and Carbon seem to be the main components, which were removed by decomposition of their carbonates and further volatilisation at temperatures below 1000 ^{o}C according to TG and in agreement with XRF and XRD analysis.

Wollastonite ($CaSiO_3$) and cuspidine ($Ca_4Si_2O_7F_2$) were the major phases encountered in the original and in the melted powder condition, respectively.

In smaller scale SiO_2, CaF_2, $CaCO_3$ and Na_2CO_3 phases were also detected in the original flux composition either by X-ray diffraction and Raman spectra. However during the melting process, as TG and DTA indicate, Na and C were decomposed, showing that only SiO_2 and CaF_2 remained.

The XRD and Micro-Raman results were in good agreement though some patterns were not available during the development of this work. Yest, their availability may confirm the presence of second phase particles in steel.

The XRF results normally used in the chemical characterization of the original powders should only be considered as a rough approximation, because during the continuous casting the melting of the powders occurs. The results indicate the formation of complex phases that might produce inclusions in steel products which could not be commercially acceptable.

The next step in the investigation is to determine which powders components minimize defects in the steel final products.

Acknowledgements

Authors thank the Brazilian Research Agency CNPq – *Conselho Nacional de Desenvolvimento Tecnológico* and FINEP for the financial support.

References

1. BRANION, R.V.; DUKELOW, D.A.; LAWSON. G.D.; SCHADE, J.; SCHMIDT, M.; TSAI, H.T. Standardized Testing of Mold Powder Properties. In: PROCEEDINGS 78th STEELMAKING CONFERENCE, 1995. Nashville, USA. Iron & Steel Society, 1995, p. 647-653.
2. CHÁVEZ, F.; RODRÍGUEZ, A.; MORALES, R.; TAPIA, V. Laboratory and Plant Studies on Thermal Properties of Mold Powders. In: PROCEEDINGS 78th STEELMAKING CONFERENCE, 1995. Nashville, USA. Iron & Steel Society, 1995, p. 679-686.
3. KASHIWAYA, Y.; CICUTTI, C.E.; CRAMB, A.W. Crystallization Phenomena of Mold Slag for Continuous Casting. ISIJ International, 38(4):357-365, 1998.
4. HILL, R.G.; DA COSTA, N.; LAW, R.V.; Characterization of a mould flux glass. Journal of Non-Crystalline Solids, 351:69-74, 2005.
5. FELDBAUER, S.; JIMBO, I.; SHARAN, A.; SHIMIZU, K.; KING, W.; STEPANEK, J.; HARMAN, J.; CRAMB, A.W. Physical Properties of Mold Slags that are Relevant to Clean Steel Manufacture. In: PROCEEDINGS 78th STEELMAKING CONFERENCE, 1995. Nashville, USA. Iron & Steel Society, 1995. p. 655-667.
6. TODOROKI, H.; ISHII, T.; MIZUNO, K.; HONGO, A. Effect of crystallization behavior of mold flux on slab surface quality of a Ti-bearing Fe–Cr–Ni super alloy cast by means of continuous casting process. Materials Science and Engineering A, 413–414:121-128, 2005.
7. EMI, T.; FREDRIKSSON, H. High-speed continuous casting of peritectic carbon steels. Materials Science and Engineering A, 413-414:2-9, 2005.
8. WINGROVE, J. Identification of iron oxides. Journal of the Iron and Steel Institute, 208(3):258-264, 1970.
9. STOFFEL, H.; FISCHER, H.; SCHULZ, K. Case study: use of the differential thermal analysis (DTA) for selective carbon-loss in casting powder mixtures. In: PROCEEDINGS OF THE 12th IAS STEELMAKING SEMINAR, 1999. Buenos Aires, Argentina, 1999, p. 429-438.
10. Cruz A, Chávez F, Romero A, Palácios E, Arrendondo V. Mineralogical phases formed by flux glasses in continuous casting mould. Journal of Materials Processing Technology, 182:358–362, 2007.
11. Choi S, Lee D, Shin D, Choi S, Cho J, Park J. Properties of F-free glass system as a mold flux: viscosity, thermal conductivity and crystallization behavior. Journal of Non-Crystalline Solids, 345-346:157-160, 2005.
12. KASHIWAYA, Y.; CICUTTI, C.E.; CRAMB, A.W. Crystallization behaviour of slags. In: PROCEEDINGS 81st STEELMAKING CONFERENCE, 1998. Toronto, Canada. Iron & Steel Society, 1998, p. 185-191.
13. FRAZEE, M.J. Standardization works on metallurgical powders. In: Report ASTM CO 8.11, 1995, p. 639-653.
14. Joint Committee on Powder Diffraction Standards. The International Centre for Diffraction Data. Available from: <http://www.icdd.com/products/overview.htm>. Access in: 05/2008.
15. NYQUIST, R.A.; PUTZIG, C.L.; LEUGERS, M.A. The handbook of infrared and Raman spectral atlas of inorganic compounds and organic salt. Academic Press, p. 1-4, 1996.